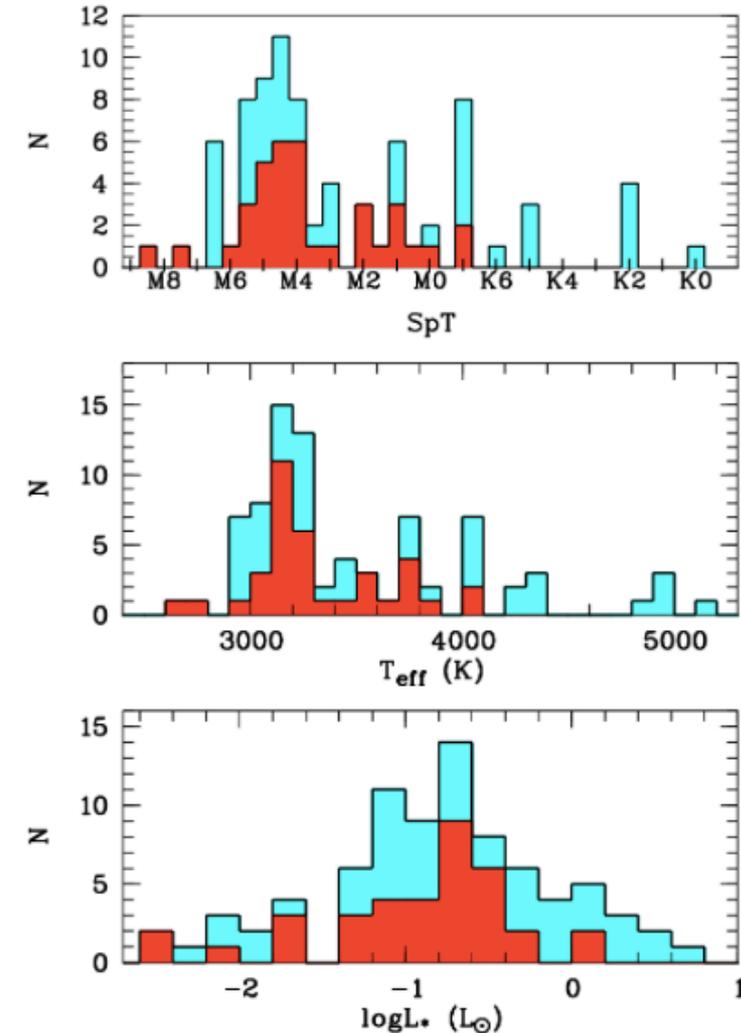


Star formation news letter # 278 1-5本目

- 大橋聡史

X-Shooter spectroscopy of young stellar objects in Lupus: Accretion properties of class II and transitional objects.

J.M. Alcalá¹, C.F. Manara², A. Natta^{3,4}, A. Frasca⁵, L. Testi^{3,6,7}, B. Nisini⁸, B. Stelzer⁹, J. P. Williams¹⁰, S. Antonucci⁸, K. Biazzo⁵, E. Covino¹, M. Esposito¹, F. Getman¹ and E. Rigliaco¹¹



Lupus I, II, III, IVのYSOをcomplete survey
81 YSOsを同定

SEDからLacc, Maccを導出し、相関を図った

SED fit

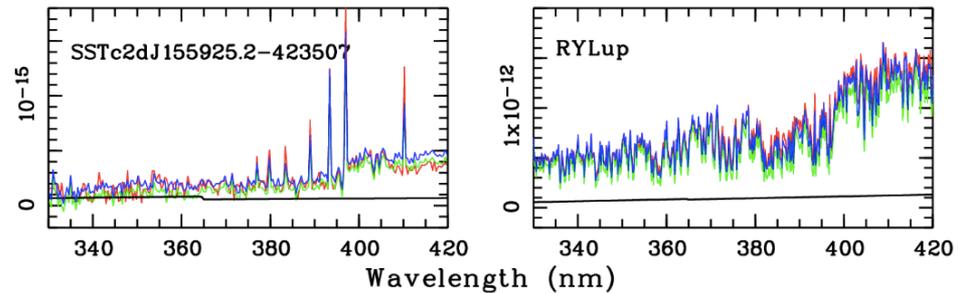
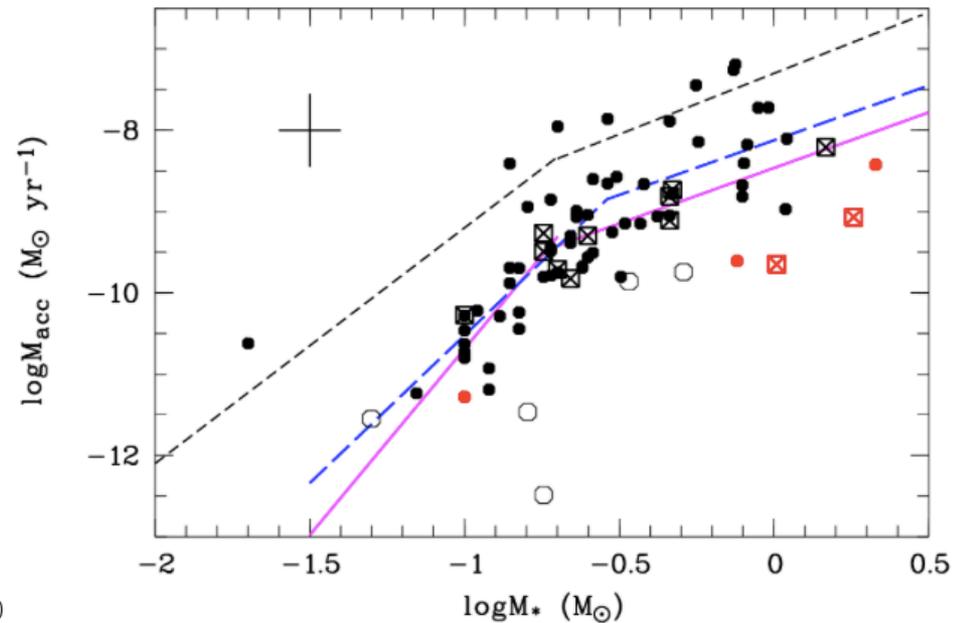
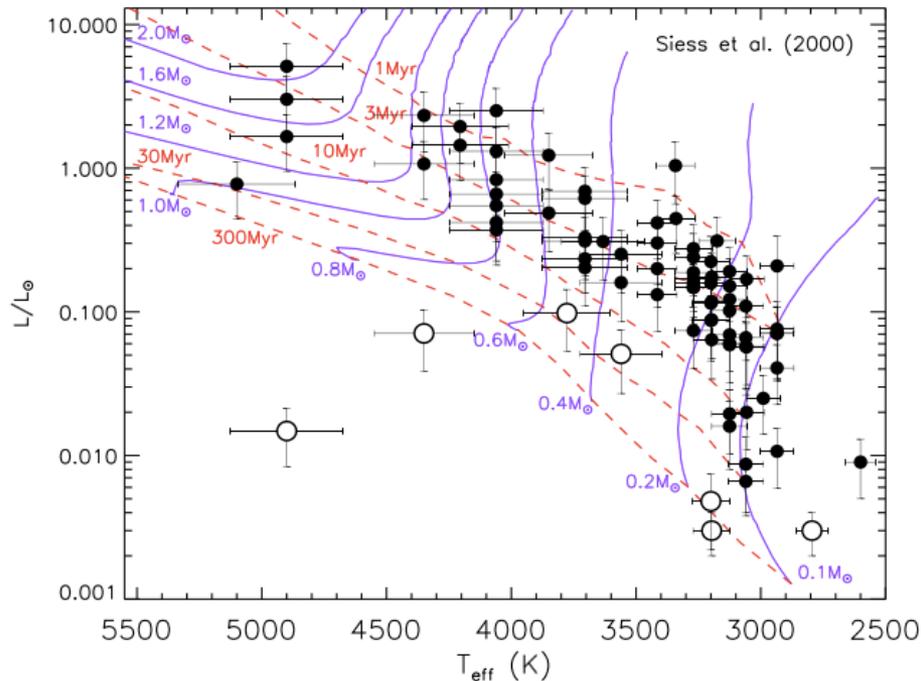


Fig. E.7. Extinction-corrected spectra (red) fitted with a combination of a photospheric template (green) and the synthetic continuum spectrum from a hydrogen slab (black). The total fit is represented with the blue line.

X-Shooter spectroscopy of young stellar objects in Lupus: Accretion properties of class II and transitional objects.

J.M. Alcalá¹, C.F. Manara², A. Natta^{3,4}, A. Frasca⁵, L. Testi^{3,6,7}, B. Nisini⁸, B. Stelzer⁹, J. P. Williams¹⁰, S. Antonucci⁸, K. Biazzo⁵, E. Covino¹, M. Esposito¹, F. Getman¹ and E. Rigliaco¹¹

<0.2 Msunでsploeのべきが変化→accretion processが違う
Massive diskは重力不安定で説明できるが、小質量側では
光乖離や惑星形成などの別のプロセスも効いてくる

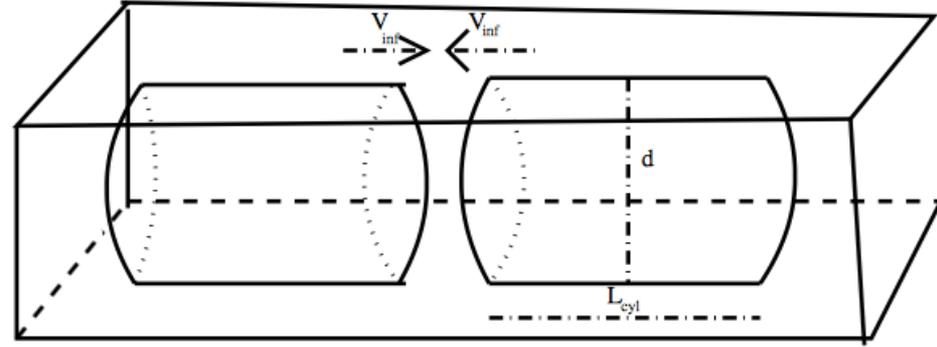


On the impact of the magnitude of Interstellar pressure on physical properties of Molecular Cloud

S. Anathpindika^{1,2}, A. Burkert^{3,4}, R. Kuiper²

Warm gasを衝突させて、
Non-linear Thin Shell Instabilityと
自己重力で分子雲を形成

SPH code SEREN



Larson's lawはvariationがあり、
外圧によって係数が変化する

Table 1. Physical details of realisations.

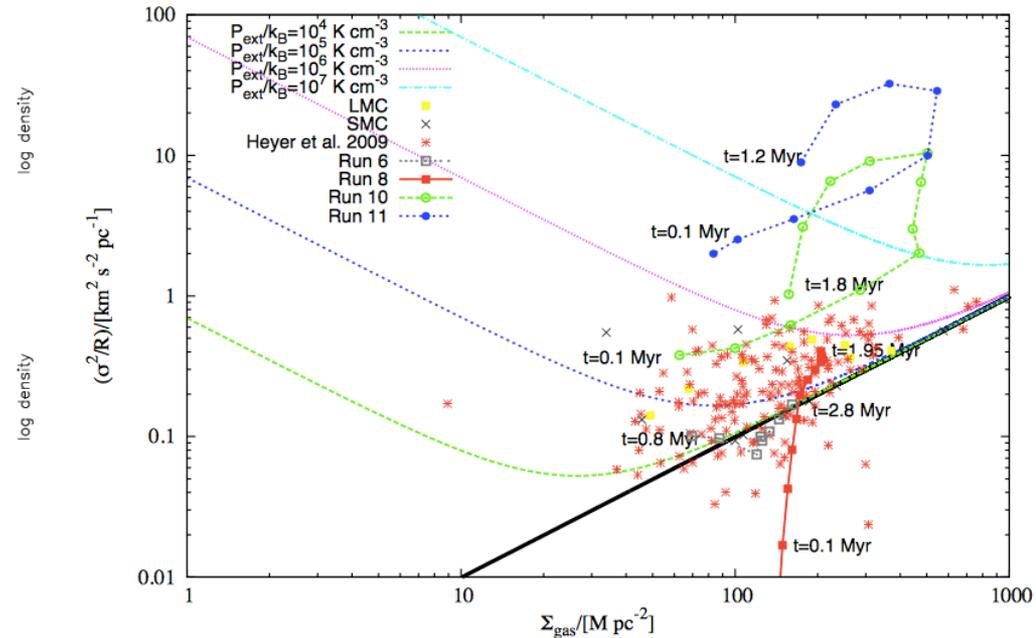
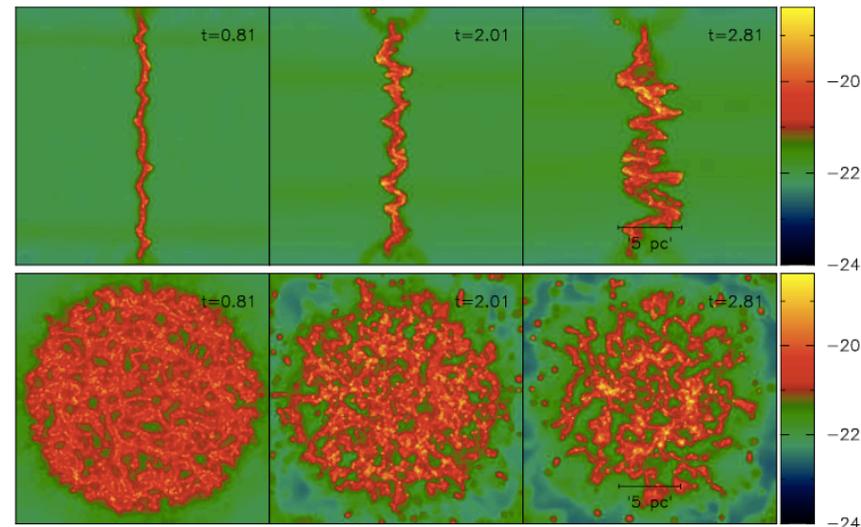
Serial No.	Physical Properties	Pre-collision Velocity of gas-flows, V_{inf} [(km/s)] Pre-collision Mach number (\mathcal{M})	$\left(\frac{P_{ext}}{k_B}\right)$ [K cm ⁻³]	M_{gas} [M _⊙]	M_{min}^a [M _⊙]	Comment
1	$L_{cyl} = 130$ pc, $R_{cyl} = 14$ pc $\bar{n} = 1$ cm ⁻³ , $T_{gas} = 5000$ K $\bar{n}_{max} \sim 10^6$ cm ⁻³ , $h_{avg}^{init} \sim 0.2$ pc	4.8 (0.7)	2.8×10^3	4.3×10^3	0.2	Warm Atomic Flow ($\mu = 1$ amu)
2	Same as (1)	9.0 (1.4)	9.8×10^3	4.3×10^3	0.2	Warm Atomic Flow
3	Same as (1)	19.28 (3.0)	4.45×10^4	4.3×10^3	0.2	Warm Atomic Flow
4	$L_{cyl} = 50$ pc, $R_{cyl} = 10$ pc $\bar{n} = 50$ cm ⁻³ , $T_{gas} = 500$ K $\bar{n}_{max} \sim 10^5$ cm ⁻³ , $h_{avg}^{init} \sim 0.13$ pc	3.45 (1.7)	7.3×10^4	4.2×10^4	2.0	Warm Atomic Flow ($\mu = 1$ amu)
5	Same as (4)	6.1 (3.0)	2.25×10^5	4.2×10^4	2.0	Warm Atomic Flow
6	Same as (4)	10.36 (5.1)	6.51×10^5	4.2×10^4	2.0	Warm Atomic Flow
7	$L_{cyl} = 30$ pc, $R_{cyl} = 10$ pc $\bar{n} = 100$ cm ⁻³ , $T_{gas} = 40$ K $\bar{n}_{max} \sim 10^4$ cm ⁻³ , $h_{avg}^{init} \sim 0.1$ pc	5.6 (15.1)	9.0×10^5	1.2×10^5	6.0	Cold Molecular Flow ($\mu = 2.29$ amu)
8	Same as (7)	7.43 (20.0)	1.6×10^6	1.2×10^5	6.0	Cold Molecular Flow
9	Same as (7)	14.86 (40.0)	6.4×10^6	1.2×10^5	6.0	Cold Molecular Flow
10	Same as (7)	29.7 (79.97)	2.56×10^7	1.2×10^5	6.0	Cold Molecular Flow
11	Same as (7)	55.6 (149.7)	8.9×10^7	1.2×10^5	6.0	Cold Molecular Flow

On the impact of the magnitude of Interstellar pressure on physical properties of Molecular Cloud

S. Anathpindika^{1,2}, A. Burkert^{3,4}, R. Kuiper²

Inflow velocityが早くなるとNTSIは早く活発になる

Dense gas を効率よくつくるにはhigh velocityでexternal pressure を上げる



EXor outbursts from disk amplification of stellar magnetic cycles

Philip J. Armitage^{1,2}

$$\beta_z \equiv \frac{P_{\text{gas}}}{B_z^2/8\pi}. \quad (1)$$

$$\alpha = 1.1 \times 10^1 \beta_z^{-0.53}. \quad (2)$$

$$P_{\text{gas}} = \rho_0 c_s^2 = \frac{1}{\sqrt{18\pi^3}} \alpha^{-1} \dot{M} \Omega^2 c_s^{-1}. \quad (3)$$

$$r_{\text{crit}} \simeq 0.095 \left(\frac{\beta_z}{10^5} \right)^{1/3} \left(\frac{B_*}{\text{kG}} \right)^{2/3} \left(\frac{r_*}{1.5r_\odot} \right)^2 \left(\frac{\alpha}{10^{-2}} \right)^{1/3} \\ \times \left(\frac{\dot{M}}{10^{-8} M_\odot \text{ yr}^{-1}} \right)^{-1/3} \left(\frac{c_s}{2 \text{ kms}^{-1}} \right)^{1/3} \text{ AU}. \quad (4)$$

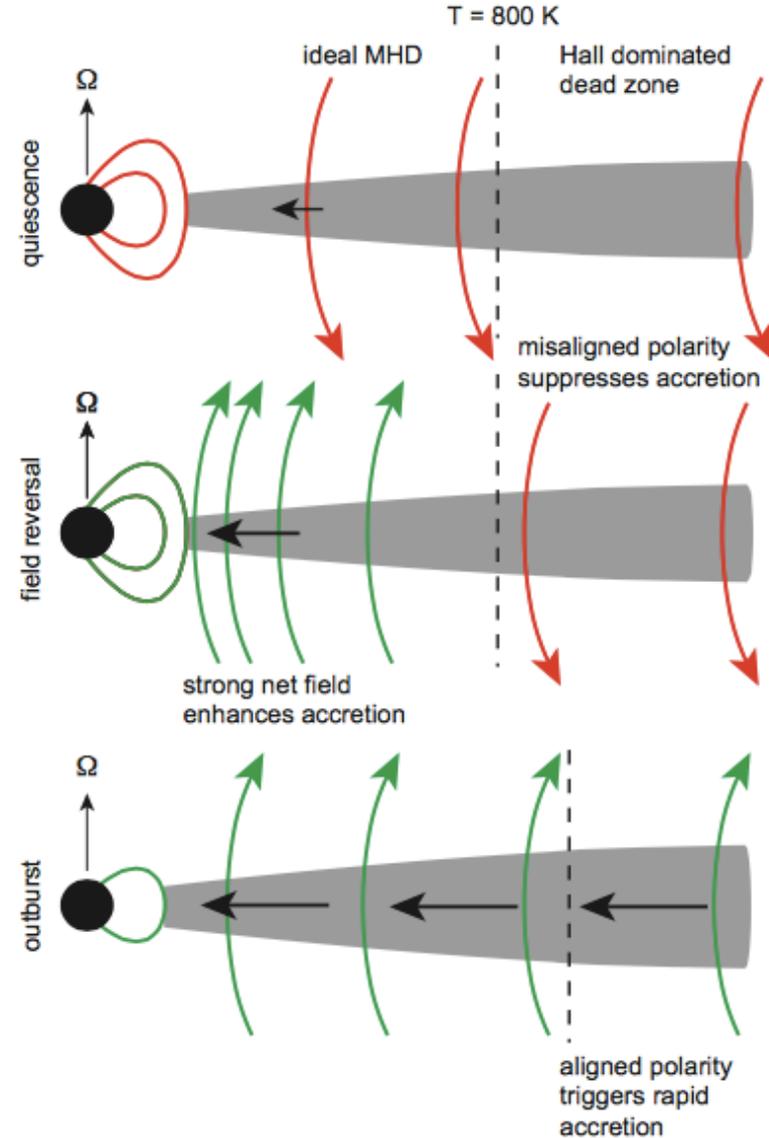
$$\Phi_{\text{open}} = 2\pi B_* \frac{r_*^3}{r_m}. \quad (5)$$

$$B_z \propto r^{-n}, \quad (6)$$

with power-law slopes,

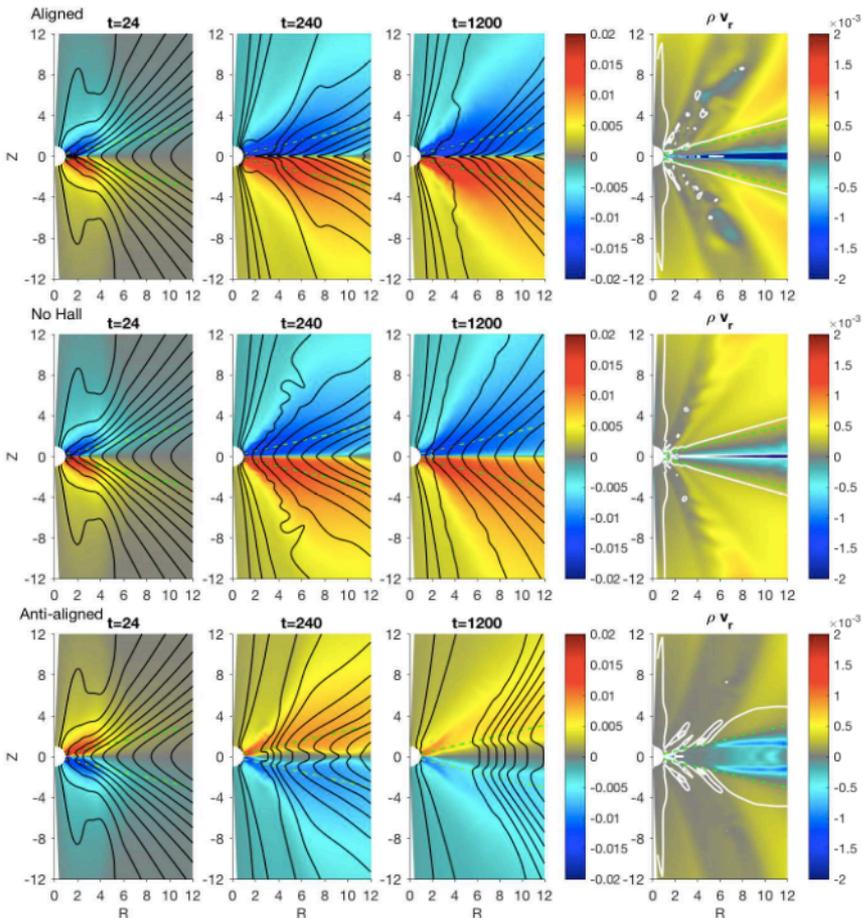
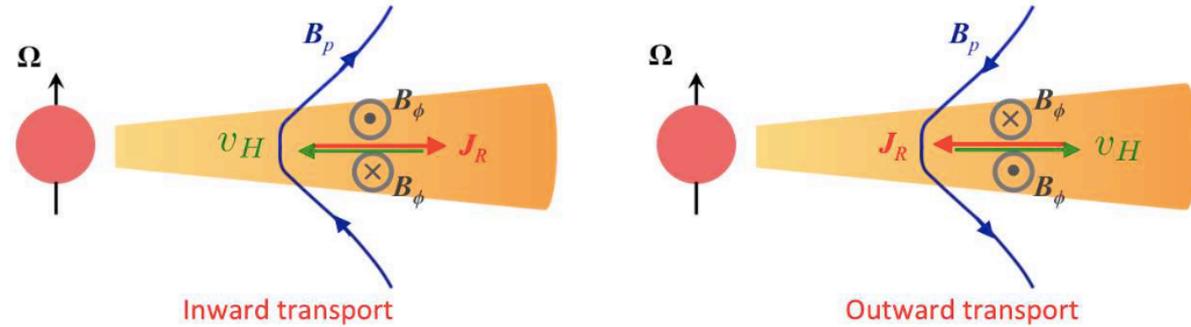
$$\begin{aligned} n=0 & \quad v_{\text{adv}}/v_{\text{diff}} \ll 1 \\ n=1 & \quad v_{\text{adv}}/v_{\text{diff}} \sim 1 \\ n=2 & \quad v_{\text{adv}}/v_{\text{diff}} \gg 1. \end{aligned} \quad (7)$$

$$\beta_z = \frac{5.6 \times 10^4}{(2-n)^2} \left(\frac{M_*}{M_\odot} \right) \left(\frac{B_*}{\text{kG}} \right)^{-2} \left(\frac{r_*}{1.5r_\odot} \right)^{-4} \\ \times \left(\frac{r_m/r_*}{10} \right)^2 \left(\frac{\dot{M}}{10^{-8} M_\odot \text{ yr}^{-1}} \right) \left(\frac{\alpha}{10^{-2}} \right)^{-1} \\ \times \left(\frac{c_s}{2 \text{ kms}^{-1}} \right)^{-1} \left(\frac{r}{0.1 \text{ AU}} \right). \quad (10)$$



Hall-effect Mediated Magnetic Flux Transport in Protoplanetary Disks

Xue-Ning Bai¹, James M. Stone²



ホール効果によって、円盤に磁場が正にalignしているとき中心へとガスは落ち込む
磁場がanti-alignだと外側へ

Hall効果とAmbipolar diffusionが影響する円盤
磁場の移動はアルフベーン速度程度

Hall-effect Mediated Magnetic Flux Transport in Protoplanetary Disks

Xue-Ning Bai¹, James M. Stone²

Hall 効果とADによってmagnetic fluxは変化、wind-drivenのaccretionはminor

Diskとpoloidal磁場がalignedの場合

Hall driftでmagnetic fluxは中へ (midplaneほど速く), upper layerはゆっくりと外側へ
これによって磁場はradial方向へ引き延ばされる(Hall shear instability)

mid planeではHall driftによる落ち込みとADによる散逸

Upper layerではHall driftとADによって散逸

Diskとpoloidal磁場がanti-alignedの場合

mid planeではHall driftで外側へ

Upper layerではpoloidal磁場が曲がり、Hall効果で外側へ

Hall(outward), AD, wind-driven accretion(inward)の全てがcontribute

Ionisation in Turbulent Magnetic Molecular Clouds

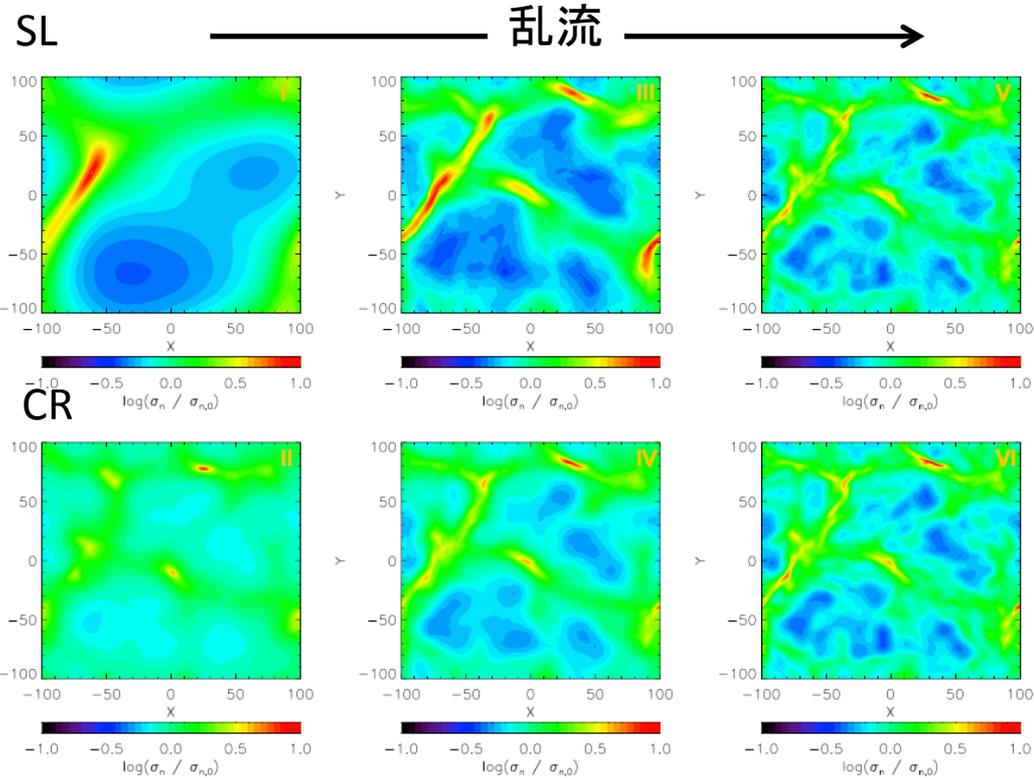
I. Effect on Density and Mass-to-Flux Ratio Structures

Nicole D. Bailey¹, Shantanu Basu² and Paola Caselli¹

磁場とionisationと乱流を入れた場合とfilament, コア形成について

$$\tau_{ni} = 1.4 \left(\frac{m_i + m_{H_2}}{m_i} \right) \frac{1}{n_i \langle \sigma w \rangle_{iH_2}}, \quad \text{AD} \quad (1)$$

Model	μ_0	v_a/c_s	$\chi_{i,0}$	Profile ^a	t_r/t_0	t_r (Myr)	$\sigma_{n,max}/\sigma_{n,0}$ ^b	μ_{max} ^b	$\mu(\sigma_{n,max})$ ^b
Set 1: Variation in Mach Number									
I	1.1	0.03		SL	81.3	31.9	10.18	1.18	1.18
II	1.1	0.03		CR	44.1	17.3	10.28	1.46	1.46
III	1.1	1.00		SL	11.3	4.4	10.46	1.25	1.20
IV	1.1	1.00		CR	7.7	3.0	10.24	1.35	1.33
V	1.1	2.00		SL	3.8	1.5	10.78	1.19	1.18
VI	1.1	2.00		CR	3.7	1.5	10.58	1.32	1.23
VII	1.1	3.00		SL	2.4	0.94	10.02	1.15	1.14
VIII	1.1	3.00		CR	2.4	0.94	10.60	1.33	1.20
IX	1.1	4.00		SL	1.8	0.71	11.54	1.16	1.14
X	1.1	4.00		CR	1.7	0.67	10.12	1.30	1.20
Set 2: Variation in Initial Mass-to-Flux Ratio									
XI	0.5	2.00		SL	> 156.5	> 61.4	3.08	0.50	0.50
XII	0.5	2.00		CR	51.5	20.2	10.11	1.62	1.62
XIII	0.8	2.00		SL	> 656.6	> 256.1	2.34	0.81	0.80
XIV	0.8	2.00		CR	17.8	7.0	10.74	1.68	1.66
XV	2.0	2.00		SL	2.7	1.0	10.50	2.05	2.05
XVI	2.0	2.00		CR	2.7	1.0	11.10	2.23	2.16

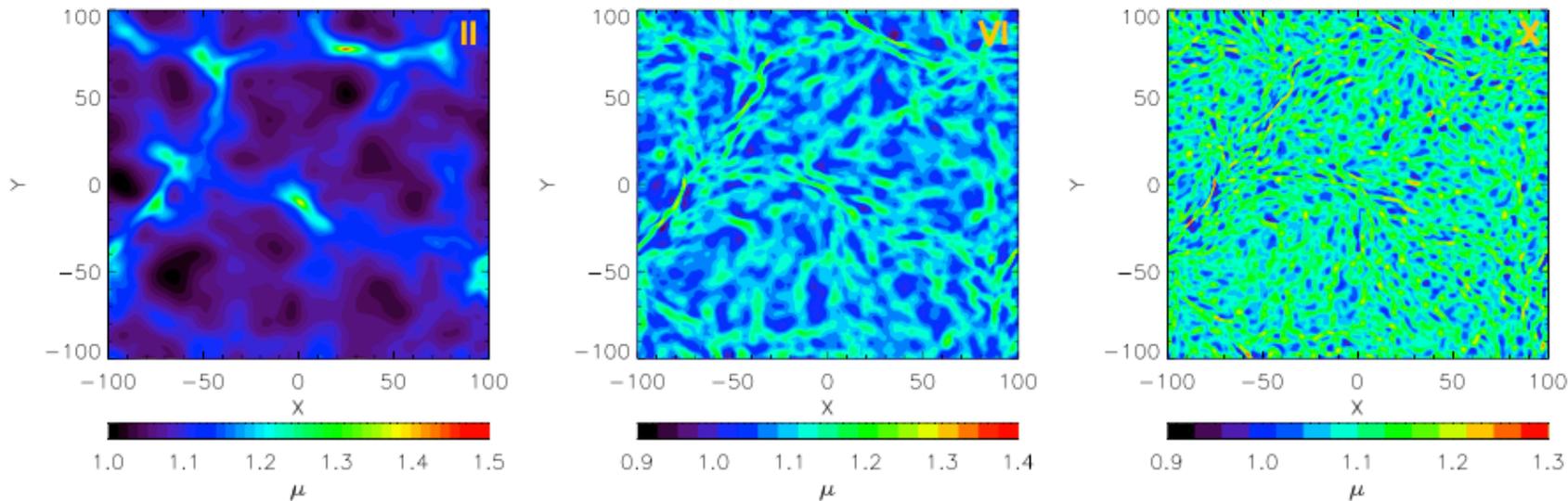


Ionisation,
乱流
Mass to flux ratioを変えてsimulation

乱流を強くするとfilamentができる
Ionisation degreeによってfilamentは依存する(あるところまで)

CR

乱流



観測されるfilamentはsupercriticalで乱流的
SLの方がcore mass は大きくなる

乱流を入れるとmass to flux ratioは
patchy, SPでより顕著

